Supplementary information

For

A comparative study on thermal- and microwave-assisted Stille-coupling polymerization of a benzodithiophene-based donor–acceptor polymer (PTB7)

Michael Ruby Raj,[‡] Minjun Kim,[‡] Hong Il Kim,[‡] Gang-Young Lee, Cheol Woong Park and Taiho Park*

Department of Chemical Engineering, Pohang University of Science and Technology, Cheongam-Ro 77, Nam-gu, Pohang, Gyeongbuk, 790-780 (Korea).

[‡] These authors contributed equally to this work.

* Corresponding author: *taihopark@postech.ac.kr*

Contents

1. Materials

2. Instruments.

3. Fabrication and characterization

4. Electrochemical properties

5. Raman spectroscopy study

Scheme S1. Mechanism of homo-coupled units (**BDT-BDT**, **FTT-FTT**) under the microwave-assisted conditions.

Fig. S1. GPC chromatograms of **T-PTB7(31k)** and **M-PTB7** polymers.

Fig. S2. TGA curves of **T-PTB7(31k)** and **M-PTB7** polymers with a heating rate of 10°C/min under N_2.

Fig. S3. DSC thermograms of **T-PTB7(31k)** and **M-PTB7** polymers with a heating and cooling rate of 10 °C/min under N_2.

Fig. S4. Cyclic voltammograms of **T-PTB7(31k)** and **M-PTB7** polymers thin films in acetonitrile solution containing 0.1 M Bu_4NPF_6 at a potential scan rate of 20 mV/s.

Fig. S5. (a) Extended Raman spectra for Peak 2 and Peak 3 of **T-PTB7(31k)** and **M-PTB7** polymers (b) Extended Raman spectra for less Raman active weak Peak 4 of **T-PTB7(31k)** and **M-PTB7** polymers.

Fig. S6. (a). Statistical analysis of (a) short-circuit current (J_{SC}), (b) fill factor (FF), (c) open-circuit voltage (V_{OC}) and (d) power conversion efficiency (PCE) depending on the PTB7-polymers.

Fig. S7. AFM topographic images of (a) **T-PTB7(31k):PC$_{70}$BM** (1:1.5 w/w %) (b) **M-PTB7(32k):PC$_{70}$BM** (1:1.5 w/w %), and (c) **M-PTB7(75k):PC$_{70}$BM** (1:1.5 w/w %) with DIO-processed. The AFM phase images of (d) **T-PTB7(31k):PC$_{70}$BM** (1:1.5 w/w %), (e) **M-PTB7(32k):PC$_{70}$BM** (1:1.5 w/w %), and (f) **M-PTB7(75k):PC$_{70}$BM** (1:1.5 w/w %) with DIO-processed. The size of images is 5 x 5 μm^2.

Fig. S8. MALDI-TOF spectrum for microwave-assisted condition generated the reaction mixture, **TIPS-BDT-FTT-BDT-TIPS** (compound **A**), **TIPS-BDT-FTT-FTT-BDT-TIPS** (compound **B**), and **TIPS-BDT-BDT-TIPS** (compound **C**).

Fig. S9. MALDI-TOF spectrum for thermal-assisted condition generated the reaction mixture, **TIPS-BDT-FTT-BDT-TIPS** (compound **A**), **TIPS-BDT-FTT-FTT-BDT-TIPS** (compound **B**), and **TIPS-BDT-BDT-TIPS** (compound **C**).

Fig. S10. Normalized UV-vis absorption spectrum for model compound **A**, compound **B** and compound **C** in the chlorobenzene solution (1x 10^{-5} M).

Table S1. Packing parameters derived from 1D GIXRD measurements.

1. Materials

The monomer of 2,6-bis(trimethyltin)-4,8-Diethylhexyloxybenzo[1,2-b;3,4-b]dithiophene (BDT) was synthesized according to a previously reported method.[1,2] The acceptor monomer of 2-ethylhexyl-4,6-dibromo-3-fluorothieno[3,2-c]thiophene-2-carboxlate (FTT) was purchased from Suna Tech Inc. All of other chemicals were used as received.

2. Instruments

Microwave irradiation polymerization reactions were performed using a "Monowave 300" single-mode microwave reactor with a maximum of 850 W magnetron output powers. ^{1}H NMR spectra were recorded on a Bruker BioSpin AG system operated at 600 MHz in deuterated chloroform solution at 298 K, unless specified otherwise. Chemical shifts (δ values) were recorded in units of ppm relative to tetramethylsilane (TMS) as an internal standard. The molecular weights of synthesized **M-PTB7** polymers and **T-PTB7** polymer were determined from calibration curve based on polystyrene standards recorded on Gel Permeation chromatography using the Shimadzu LC solution at a flow rate of 1.0 mL/min chlorobenzene solution at 40 ^{o}C. Thermogravimetric analysis (TGA) were performed with TG/DTA Q500 (TA Instrument) at a heating rate of 10 °C/min ramp from 50 to 900 °C under a nitrogen atmosphere. Differential scanning calorimetric (DSC) measurements of **T-PTB7(31k)** (sample wt: 4 mg) and **M-PTB7** polymers (samples wt: 4 mg) were performed using a Perkin-Elmer Pyris DSC 4000 instrument under a nitrogen atmosphere at a heating and cooling rate of 10 ^{o}C/min. Elemental analysis for all **PTB7** polymers were performed using a Thermofinnigan EA 2000 CHNS analyzer and Thermofinnigan EA1112 Oxygen analyzer under argon atmosphere. UV-Vis absorption spectrum and photoluminescence (PL) spectrum of **T-PTB7(31k)** polymer and **M-PTB7** polymers solutions recorded using an OPTIZEN POP UV-Vis double beam spectrometer and Jasco FP-6500 spectrometer, respectively. Electrochemical cyclic voltammetry (PowerLab/AD instrument model system) were recorded in a computer controlled potentiostat conventional three-electrode system in polymer thin films using a glassy carbon disk as the working electrode, platinum-wire as the counter electrode, and silver wire as the quasi-reference electrode in a acetonitrile (AN, HPLC grade) solution containing 0.1 M tetrabutylammonium hexafluorophosphate (Bu4NPF6) as supporting electrolyte at a scan rate of 20 mV/s. Ferrocene is used as internal standard to calculate frontier orbital energy levels of polymers. Raman spectroscopy measurements were carried out for all polymer thin films using a Renishaw inVia microscope with a 50× objective in a back-scattering configuration. The excitation source was a 488 nm (Ar ion) laser, spectra were obtained with a laser power of ~0.9 mW and an acquisition time of 60 s in an N_2 environment. Grazing-incidence XRD (GIXD) measurements were performed at the 5A XRS beamline

($\lambda \approx 1.07$ Å), with an incident energy of 11.56 keV, at the Pohang Accelerator Laboratory (PAL). The X-ray incident angle was fixed at 0.2° to maximize the diffracted signal and minimize the background from substrate scattering. Topographic images of the neat polymers (**T-PTB7(31k)**, **M-PTB7(32k)**, **M-PTB7(75k)**) and polymer:$PC_{70}BM$ films (surface area: 5 x 5 μm^2) were recorded using a digital Nanoscope III atomic force microscope operated in the tapping mode under ambient conditions. Films were prepared by dissolving **T-PTB7(31k)** and **M-PTB7** polymers and **$PC_{70}BM$** in chlorobenzene and followed by spin-coating on the top surface of a glass substrate. The prepared samples were annealed at 120 °C on a hot plate under nitrogen before measurement. MALDI-TOF mass spectroscopic analyzes were recorded on a Bruker Daltonics UltrafleXtreme MALD-TOF system, a Relative positive method (RP) using dithranol as matrix (10 mg in 0.5 mL of DCM).

3. Fabrication and characterization

Solar cell devices were fabricated on 2.5 x 2.5 cm pre-patterned ITO-glass substrates. The ITO-glass substrates were washed using detergent, deionized water (DI-water), acetone and isopropyl alcohol (IPA). After washing, the ITO coated glass substrates were dried in the 140°C oven overnight. The ITO coated glass substrates were treated with the UV-ozone for 15 mins. The sol-gel of ZnO solution was prepared with zinc acetate dehydrate ($Zn(CH_3COO)_2 \cdot 2H_2O$, Aldrich, 99.9%, 1g) and Ethanolamine ($NH_2CH_2CH_2OH$, Aldrich, 99.5%, 0.28g) dissolved in 2-methoxyethanol ($CH_3OCH_2CH_2OH$, Aldrich, 99.8%, 10mL) under vigorous stirring for 12 h, 60°C, hydrolysis reaction in the air. The ZnO sol-gel solution was spin-coated at 5000 rpm for 30 seconds on the pre-cleaned ITO-glass substrate. The films were heated at 200°C for 1 h in air, and then the devices were transferred to a glove box. A solution containing the blend of PTB7:$PC_{70}BM$ (1:1.5, weight ratio) in chlorobenzene with 3 vol% diiodooctane (DIO) was spin-coated at 1200 rpm for 30 seconds on the ZnO (~100 nm). Then, the samples were dried overnight under nitrogen atmosphere at room temperature. Finally, to complete the devices, MoO_3 (20 nm) and Ag (100 nm) layers were thermally evaporated with a shadow mask under high vacuum (less than 10-6 Torr). The active area of the fabricated device was 0.04 cm^2. Using a Keithley 2400 SMU and an Oriel xenon lamp (450 W) with an AM1.5 filter, the solar cells were characterized in air under AM 1.5G illumination of 100 mW/cm^2 (Oriel 1 kW solar simulator), which was calibrated with a KG5 filter.

4. Electrochemical Properties

The electrochemical properties of **T-PTB7(31k)** and **M-PTB7** polymers were determined using cyclic voltammeter on the thin film as shown in Fig. **S4** and the overall results were summarized in **Table 1**. The position of HOMO and LUMO energy levels of all **PTB7** polymers were estimated from onset point of oxidation potential and optical band gap of corresponding polymer in thin film, respectively. From Table 1, it can be seen that **M-PTB7** polymers from **M-PTB7(32k)** to **M-PTB7(75k)** show the high-lying HOMO energy level as compared to that of **T-PTB7(31k)**, whereas the LUMO energy levels were decreased. This result indicates that the homo-coupled units in the main chain of **M-PTB7** polymers could acts as lower lying energy trapping sites results in high-lying HOMO energy levels and decreased the LUMO energy levels.[3]

5. Raman Spectroscopy study

We used Raman spectroscopy method to sense the existence of homo-coupled units and its origin of Raman vibrational modes in **M-PTB7(32k)** (Fig. 2d). From Fig. 2d, both **T-PTB7(31k)** and **M-PTB7(32k)** polymers exhibited a distinctive Raman spectrum with four major peaks from vibrational modes of the common features of **PTB7**. In case of **T-PTB7(31k)**, **Peak 1** (~1498 cm^{-1}) was attributed due to the C=C stretching mode of **BDT** unit's fused thiophenes, **Peak 2** (~1553 cm^{-1}) was assigned due to a coupled vibration of the identical mode to the C=C stretching mode of non-fluorinated thiophene of **TT** unit, **Peak 3** (~1575 cm^{-1}) was ascribed due to a quadrant stretching mode attached to the C=C stretching mode of the fluorinated thiophene of **TT**. A weak **peak 4** at ~1708 cm^{-1} was associated to the less Raman-active C=O stretching mode of **TT** unit's side chain of ester groups. The Raman bands arises from 1200 to 1360 cm^{-1} were assigned due to the stretching mode of phenylene-alkoxy (R-O) group in **BDT** unit.[4,5] Although **T-PTB7(31k)** and **M-PTB7(32k)** showed nearly similar the shape of C=C and C=O stretching vibrational modes, they exhibited little difference in Raman vibrational modes (Fig. S5a and S5b). However, **M-PTB7(75k)** showed remarkable difference in the Raman vibrational modes (Fig. 2d) in terms of (i) decreased the intensity of **Peak 1** with ~4 cm^{-1} shifted to higher wavenumbers, (ii) increased the intensity of **Peak 2** with ~5 cm^{-1} shifted to higher wavenumbers, and (iii) little changes in **Peak 3** as well as in Raman less weak **Peak 4** of Raman vibrational modes of **M-PTB7(75k)**, indicating the C=C bonds for (i) fused thiophene of **BDT** units (Peak 1), (ii) non-fluorinated thiophene (Peak 2), (iii) fluorinated thiophene of **TT** units (Peak 3), and (iv) less Raman-active C=O bonds of **TT** unit's side chain of ester groups (weak Peak 4) were vibrating at higher frequency. From these results, we speculated that the existence of homo-coupled units such as **BDT-FTT-FTT** (Fig. 2b) unit and **BDT-BDT** (Fig. 2c) unit in the main chain of **M-**

PTB7(75k) polymers induced polymer aggregation which led to significant change in the Raman peaks intensity as well as shifted to higher wavenumbers as compared to **T-PTB7(31k)**. These effects originated from decreased intra- and intermolecular interaction and decreased conjugation lengths in **M-PTB7(75k)** thin film. Thus, this finding clearly provides the evidence that synthesized **PTB7** (**M-PTB7** polymers) by microwave-assisted Stille cross-coupling polymerization method generates a existence of **BDT-FTT-FTT** as well as **BDT-BDT** units. Furthermore, the noticeable difference between the Raman spectrum of **T-PTB7(31k)** and **M-PTB7** polymers (Fig. 2d) clearly suggested that **PTB7** (**T-PTB7(31k)**) prepared by thermal condition is virtually free from such a kind of homo-coupled units.

Scheme S1. Mechanism of homo-coupled units (**BDT-BDT**, **FTT-FTT**) under the microwave-assisted conditions.

Fig. S1. GPC chromatograms for **T-PTB7(31k)** and **M-PTB7** polymers.

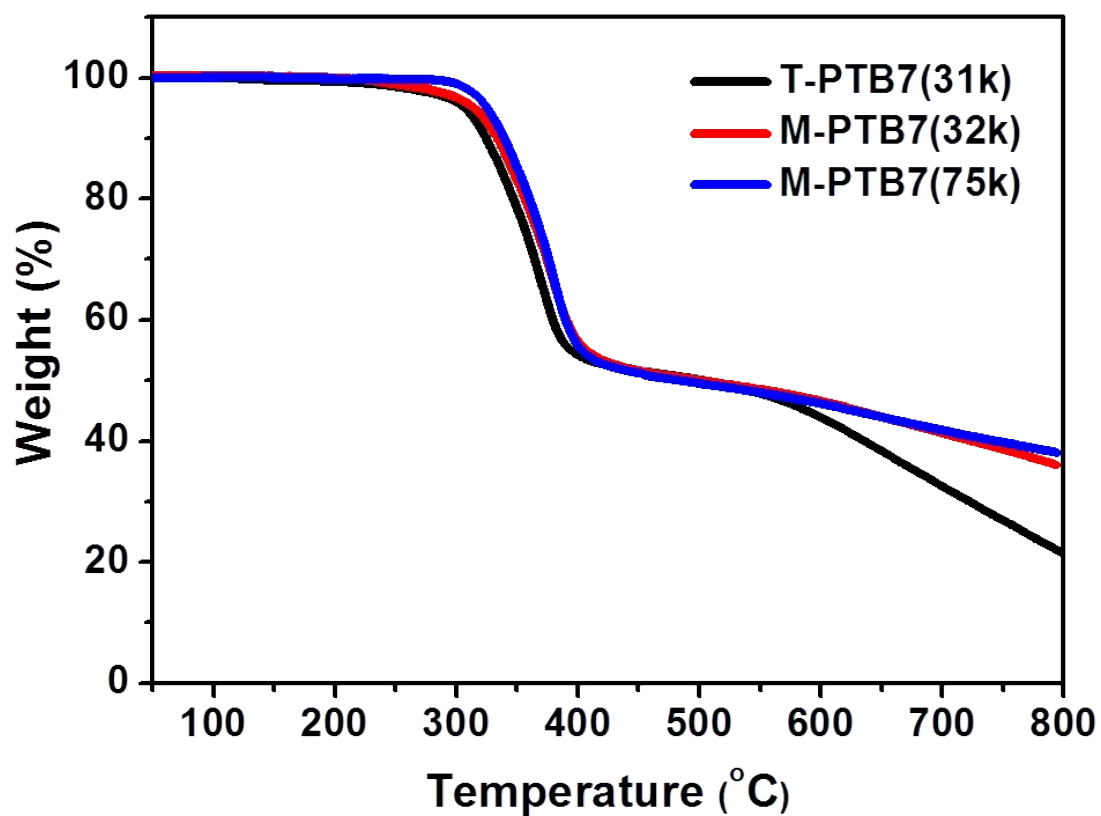**Fig. S2**. TGA curves of **T-PTB7(31k)** and **M-PTB7** polymers with a heating rate of 10°C/min under N_2.
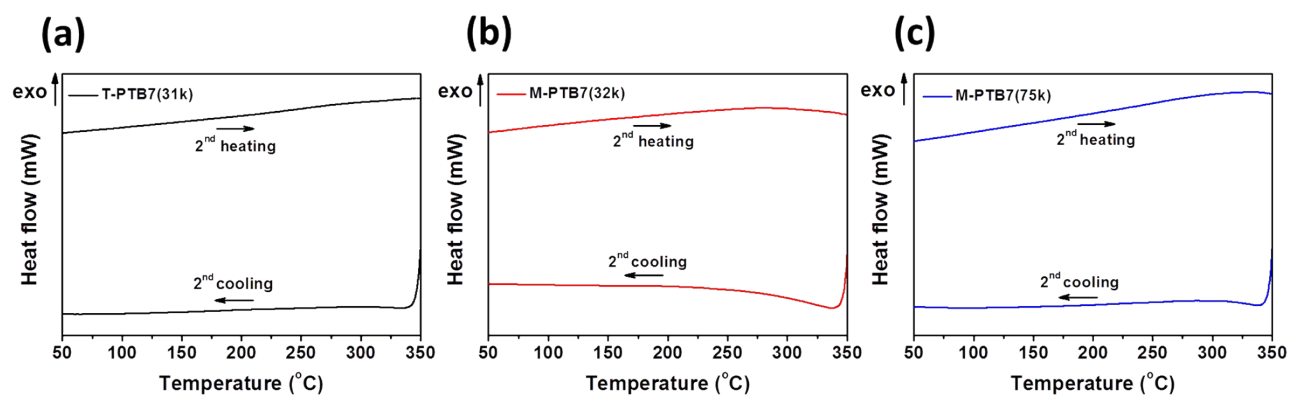
Fig. S4. Cyclic voltammograms for **T-PTB7(31k)** and **M-PTB7** polymers thin films in acetonitrile solution containing 0.1 M Bu_4NPF_6 at a potential scan rate of 20 mV/s.
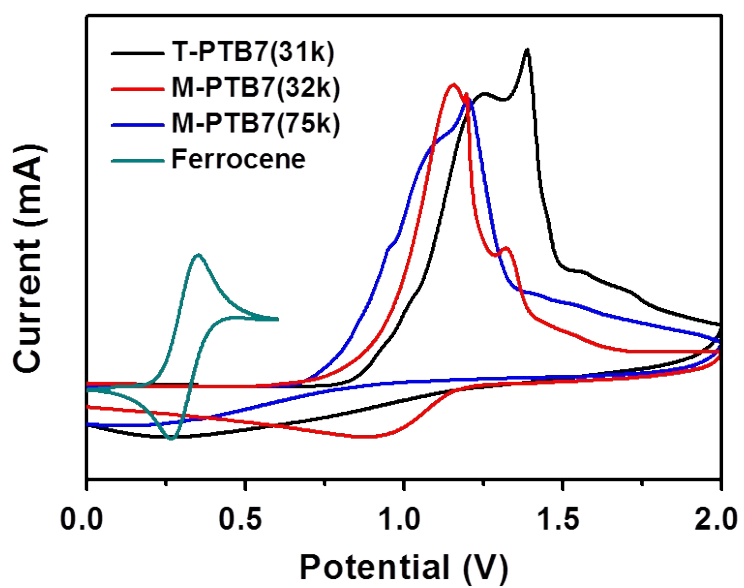
Fig. S5. (a) Extended Raman spectra for Peak 1, Peak 2 and Peak 3 of **T-PTB7(31k)** and **M-PTB7** polymers (b) Extended Raman spectra for less Raman active weak Peak 4 of **T-PTB7(31k)** and **M-PTB7** polymers.
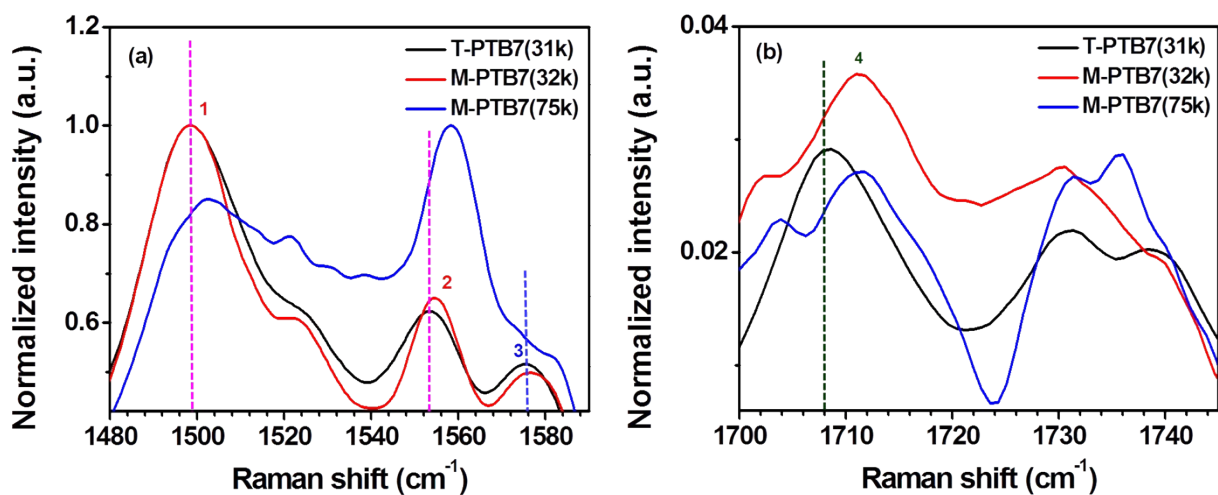
Fig. S6. (a). Statistical analysis of (a) short-circuit current (J_{SC}), (b) fill factor (FF), (c) open-circuit voltage (V_{OC}) and (d) power conversion efficiency (PCE) depending on the PTB7-polymers.
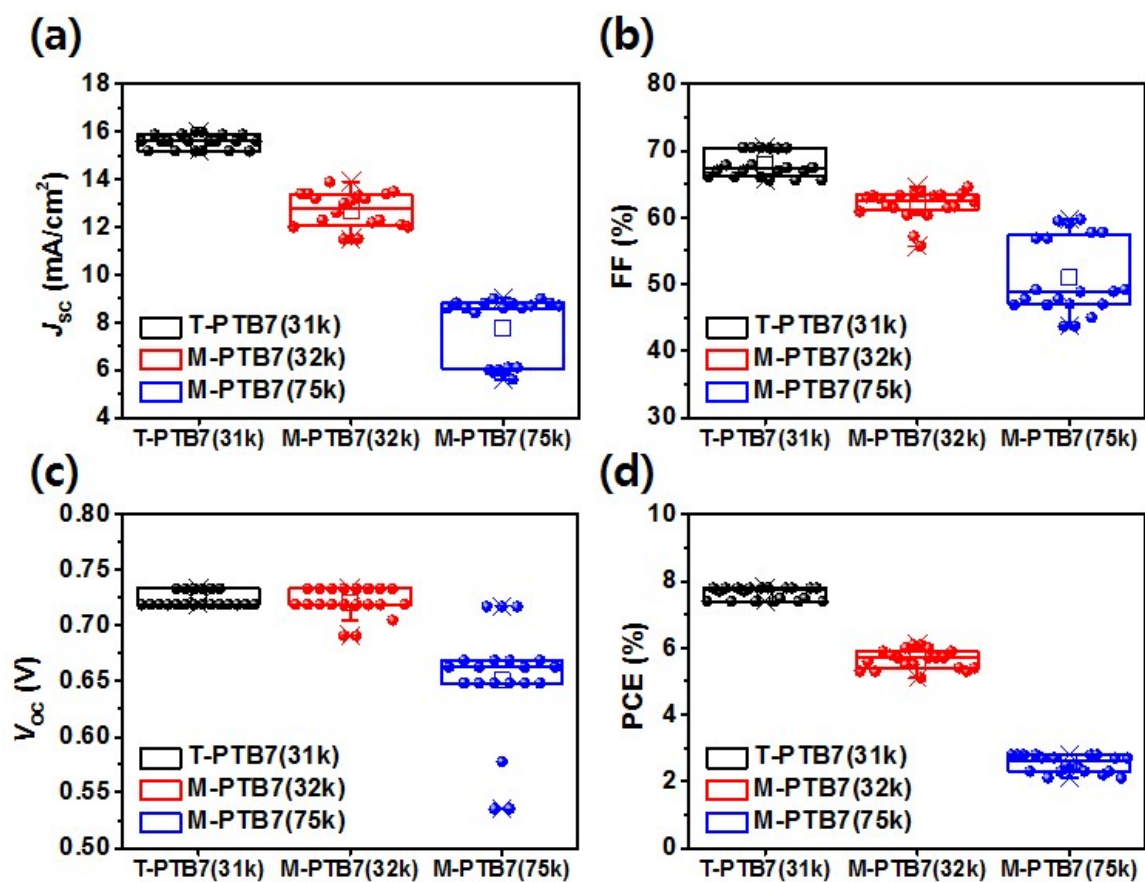
Fig. S7. AFM topographic images of (a) **T-PTB7(31k):PC$_{70}$BM** (1:1.5 w/w %) (b) **M-PTB7(32k):PC$_{70}$BM** (1:1.5 w/w %), and (c) **M-PTB7(75k):PC$_{70}$BM** (1:1.5 w/w %) with DIO-processed. The AFM phase images of (d) **T-PTB7(31k):PC$_{70}$BM** (1:1.5 w/w %), (e) **M-PTB7(32k):PC$_{70}$BM** (1:1.5 w/w %), and (f) **M-PTB7(75k):PC$_{70}$BM** (1:1.5 w/w %) with DIO-processed. The size of images is 5 x 5 µm^2.
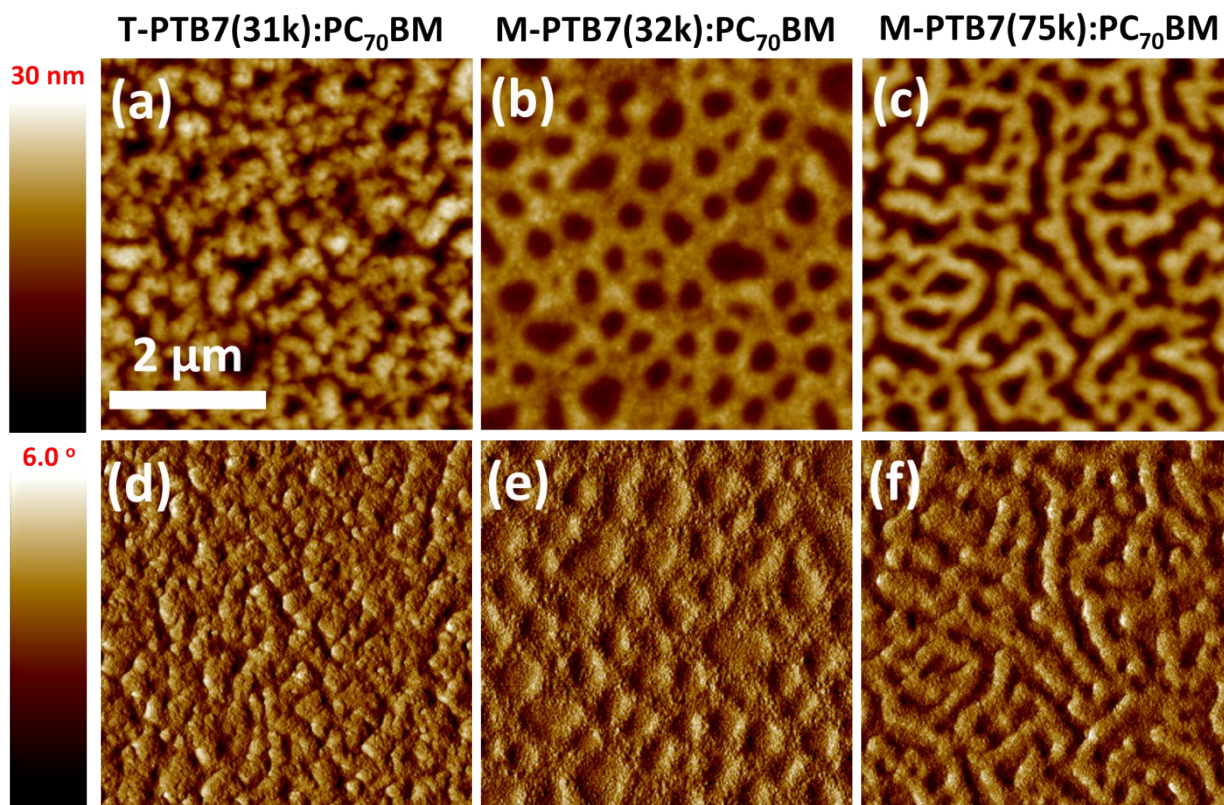
Fig. S8. MALDI-TOF spectrum for microwave-assisted condition generated the reaction mixture, **TIPS-BDT-FTT-BDT-TIPS** (compound **A**), **TIPS-BDT-FTT-FTT-BDT-TIPS** (compound **B**), and **TIPS-BDT-BDT-TIPS** (compound **C**).
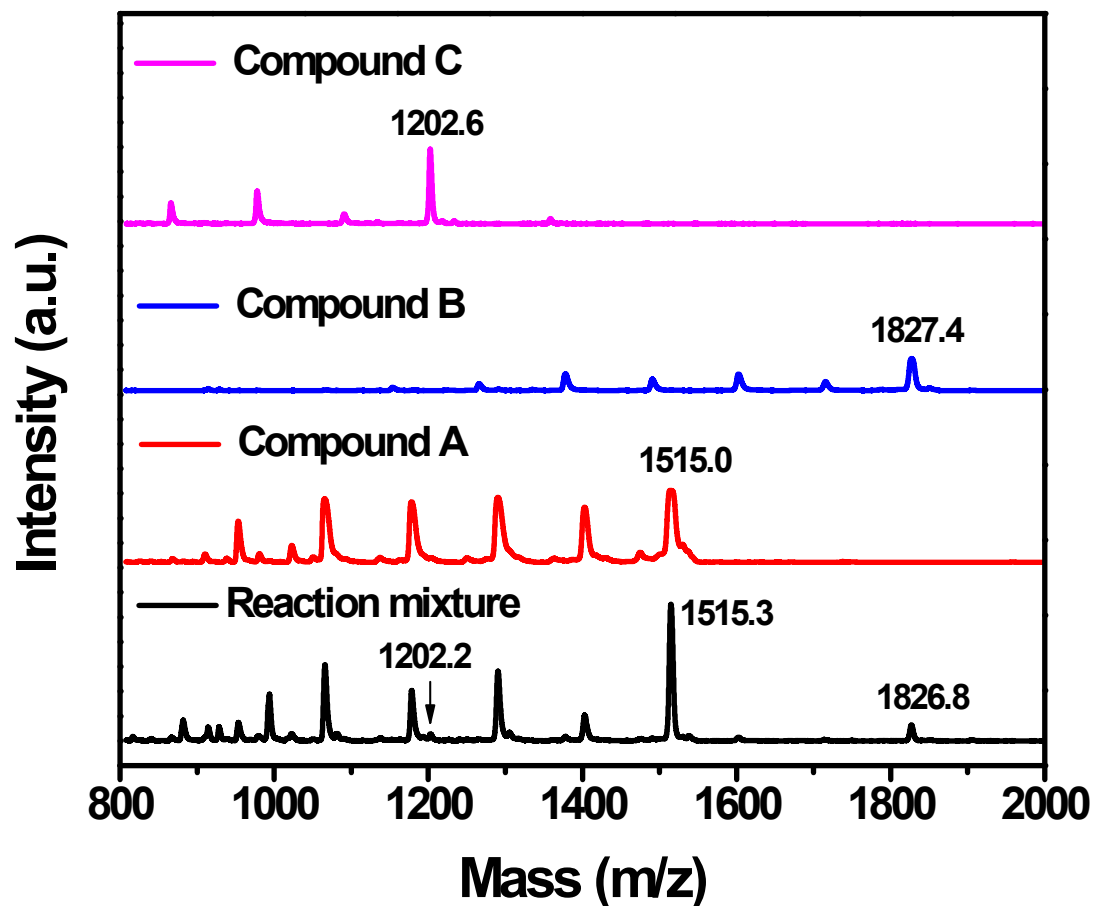
Fig. S9. MALDI-TOF spectrum for thermal-assisted condition generated the reaction mixture, **TIPS-BDT-FTT-BDT-TIPS** (compound **A**), **TIPS-BDT-FTT-FTT-BDT-TIPS** (compound **B**), and **TIPS-BDT-BDT-TIPS** (compound **C**).
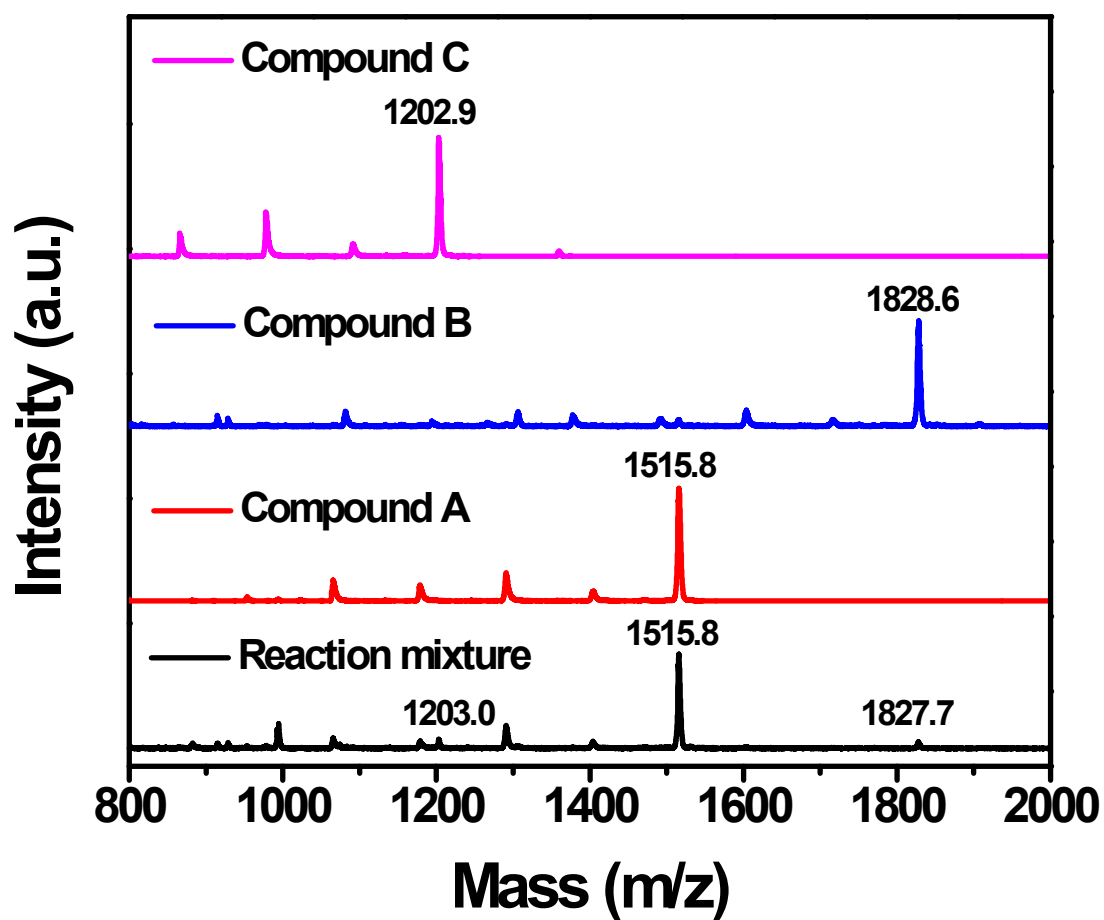
Fig. S10. Normalized UV-vis absorption spectrum for model compound **A**, compound **B** and compound **C** in chlorobenzene solution (1x 10^{-5} M).
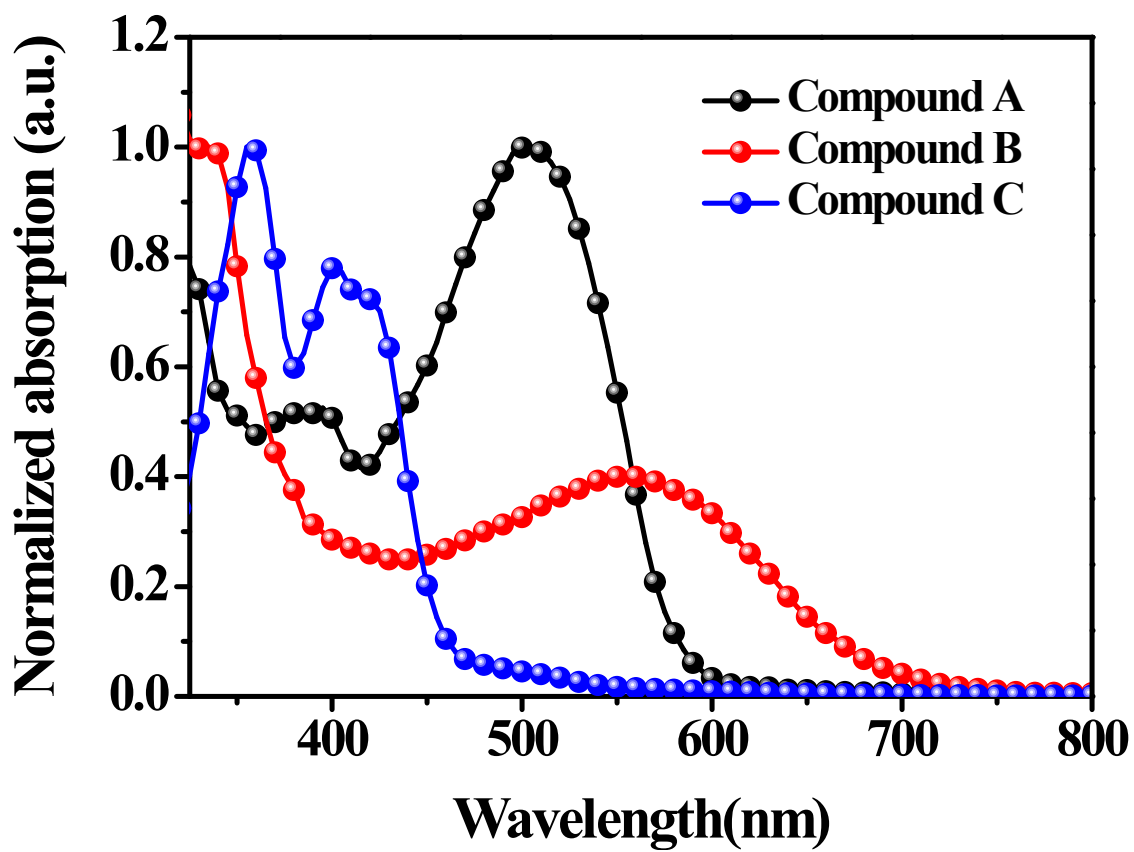
Table S1. Packing parameters derived from 1D GIXRD measurements.

Films	Crystallographic parameters			
	Lamellar spacing (In-plane direction)		π-π stack distance (Out-of-plane direction)	
	q_{xy} (nm^{-1})	d-spacing (nm)	q_z (nm^{-1})	d-spacing (nm)
T-PTB7(31k)	3.22	1.95	16.17	0.39
M-PTB7(32k)	3.12	2.01	16.12	0.39
M-PTB7(75k)	2.97	2.11	16.02	0.39
T-PTB7(31k):PC$_{70}$BM blend	3.53	1.78	16.02	0.39
M-PTB7(32k):PC$_{70}$BM blend	3.27	1.92	15.92	0.39
M-PTB7(75k):PC$_{70}$BM blend	3.17	1.98	15.92	0.39

References

[1] J.-H. Kim, H. U. Kim, C. E. Song, I. -N. Kang, J. -K. Lee, W. S. Shin, D.-H. Hwang, Sol. Energy Mater. Sol. Cells 108 (2013) 113–125.

[2] J. Hou, H.-Y. Chen, S. Zhang, Y. Yang, J. Phys. Chem. C 113 (2009) 21202–21207.

[3] F. J. Lim, A. Krishnamoorthy, G. W. Ho, ACS Appl. Mater. Interfaces 7 (2015) 12119−12127.

[4] S. Chambon, A. Rivaton, J. L. Gardette, M. Firon, Sol. Energy Mater. Sol. Cells 92 (2008) 785−792.